Passive RF Observations of Cislunar Objects

Thomas Joyce
Lunar and Planetary Laboratory, Department of Astronomy, Department of Physics, University of Arizona
Ryland Phipps
Department of Aerospace and Mechanical Engineering, University of Arizona
Craig Jacobson
Lunar and Planetary Laboratory, University of Arizona,
Tanner Campbell
Department of Aerospace and Mechanical Engineering / Lunar and Planetary Laboratory, University of Arizona
Adam Battle
Lunar and Planetary Laboratory, University of Arizona
Dr. Daniel Estévez
Independent Researcher, Spain
Prof. Roberto Furfaro
Department of Systems and Industrial Engineering, Department of Aerospace and Mechanical Engineering, University of Arizona
Prof. Vishnu Reddy
Lunar and Planetary Laboratory, University of Arizona

ABSTRACT

Cislunar observations are becoming increasingly important as more attention is dedicated to lunar operations. With the technique of passive radio frequency observations (passive RF) there exists the capability to detect, track, and identify space to ground communication signals from cislunar objects. Using a 0.6-meter S-Band parabolic reflector antenna, a survey was conducted that included observations of five cislunar targets. These targets were successfully found and a detection flux threshold of $1.03 \cdot 10^{-16}\, W/m^2$ was derived for the system. The objective of this study was to determine the efficacy of passive RF detections for the tracking of Earth and lunar orbiting satellites. This survey was successful, and the implementation of new hardware will allow for cislunar tracking to become viable.

1. INTRODUCTION

Cislunar space is a major topic in the field of Space Situational Awareness (SSA) as the orbital region around the Moon is rapidly becoming an area for development and activity. For example, in August 2022 South Korea began its first lunar mission with the launch of its Korean Pathfinder Lunar Orbiter (KPLO) spacecraft [1]. Subsequently in November 2022 NASA launched its Artemis I Spacecraft [2], as a spearhead of their new Lunar Gateway program [3]. Furthermore, India also continued its Chandrayaan program by launching its third iteration, Chandrayaan-3 in July 2023 [4]. With all this new attention being focused on the lunar orbital region, the process of tracking and managing the trajectories of these objects is of great importance.

Lack of effective space traffic management has been seen clearly in Low Earth Orbit (LEO), as this regime suffers from congestion [5]. While the LEO regime may already be compromised, it is imperative that other orbital domains do not follow the same fate. Yet detecting and tracking in lunar space can prove difficult, as objects can appear faint in the optical wavelengths and depending on the object's angular separation from the Moon and Sun, the background could be bright enough to make such observations impossible. Luckily, the optical wavelengths are only a small sliver of the electromagnetic spectrum, allowing observers here on Earth to track these lunar targets by other means, utilizing alternative wavelength ranges.

Passive RF is a methodology that harnesses the power of low-attenuating space-to-Earth radio communications to passively track satellites communicating with the Earth. In contrast to radar which requires an active transmission and reflection signal, passive RF is able to receive and interpret signals emitting from an operational satellite, requiring no ground-based transmission for the observation to occur.

This method has a variety of competitive advantages that expand the opportunities of ground-based observations. With this technique, angular position and velocity estimations can be obtained. Additionally, these observations have the flexibility to be performed regardless of the time of day and during non-optimal atmospheric conditions, such as inclement weather. Given the right orbital geometry and transmission schedule, passive RF observation can enable the possibility for upwards of 24-hour coverage of a specified target.

Passive RF can also suffer from disadvantages that can hinder or prevent detections of certain objects. As each object emits its own frequency, there can be some bands, or regions of the electromagnetic spectrum, that are unavailable to the observer. This research was completed using a subset of the S-band frequency range of 2.1 to 2.5 GHz. Without investment in alternative systems, detections of the X-band (8 - 12 GHz) for instance will not be available. These observations are also limited to the time at which the object is emitting a communication signal. If telemetry or science data is not being sent down to Earth, it cannot be collected and the object cannot be tracked, creating a window of halted tracking. In addition, the beam width of our small passive RF system is large, resulting in coarse astrometry compared to similar aperture optical systems. For example, our 0.6-meter S-band system has a beamwidth of 17.22 degrees at 2.1 GHz [6] whereas a comparable optical system is capable of producing sub-arc second astrometry.

Overall, passive RF is best combined with optical observations so that both methods can be utilized in tandem to provide substantial tracking capability. An observation network that features both methods can be flexible to variances in observation conditions such as poor weather, phase angle dimming, unknown transmission schedules, and maneuvers empowering more reliable follow-up tracking.

We present the academic implementation of this method, with our lab's newly established Passive RF tracking station. Using the hardware available, a survey was conducted featuring the successful observations of five lunar orbiting targets and the determination of a detection threshold.

2. OBSERVATIONS

Observations of five cislunar targets were performed on six separate frequencies, as summarized in table 1. In each occurrence the signal received had a very narrow bandwidth, on the order of a few kilohertz. This implies we likely detected signals consisting of residual carrier modulation, telemetry, or instrument status information [7]. Science data is typically transmitted as larger bandwidth signals to accommodate the additional information present in these data sets.

Table 1. Observational circumstances for detection of five cislunar targets.

Name of Spacecraft	Country of Origin (Space Agency)	Date and time of detection (in UTC)	Frequency of Detection	Signal to Noise Ratio (SNR)
Artemis-1	U.S.A. (NASA)	11/28/2022, 23:24	2.22009 GHz	10 dB
KPLO	South Korea (KARI)	11/28/2022, 22:48	2.26080 GHz	17 dB
LRO	U.S.A. (NASA)	7/6/2023, 06:52	2.27121 GHz	10 dB
Queqiao	China (CNSA)	7/6/2023, 06:56	2.28700 GHz	17 dB
Queqiao	China (CNSA)	7/6/2023, 07:22	2.23452 GHz	4 dB
Chandrayaan-2 (Orbiter)	India (ISRO)	7/6/2023, 07:11	2.23977 GHz	8 dB

3. METHODOLOGY

Our passive RF observations were conducted using a methodology that allowed for repeatability. The first step involves observation planning to determine the target's downlink frequencies and sky position at the time of observation. When conducting these observations, calibration targets are used to optimize the system for maximum data collection. These calibration targets are defined as strong, consistent emitters like satellite radio sources in GEO. These calibrations are necessary as localized noise conditions can fluctuate from day to day and depending on the observation site. Next, data is collected from the selected target to determine its magnitude, as well as the magnitude of the adjacent frequency ranges. This allows for the determination of the signal-to-noise ratio (SNR) to quantify the strength and uncertainty of the signal detection. In this stage the settings used are documented for data processing at a later stage, along with the angular position for tracking and orbit determination. These steps are summarized in Fig. 1.

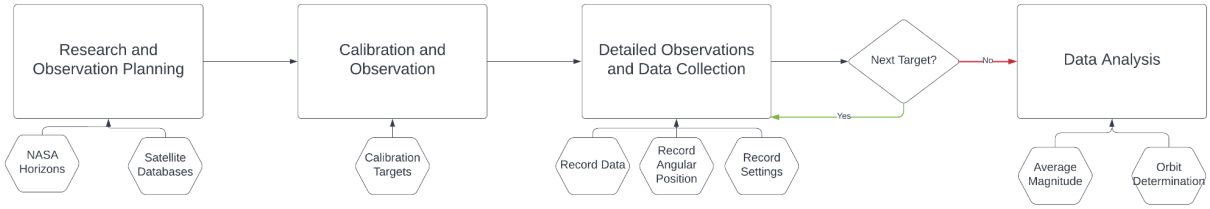

Fig. 1. Flow graph displaying steps used in the passive RF observation process

The output of the FFT recorded data is in the form of complex pairs. The data recordings of the signals are taken at an interval of 20 seconds with a fixed sample rate. The signal magnitude is estimated by comparing the magnitude of the signal to the surrounding noise floor. The SNR is calculated using a bandwidth of 244.1 Hz to determine the strength of the signal compared to the surrounding noise floor within this frequency bin.

The detection threshold was acquired by observing the signal in tandem with NASA's deep space network (DSN). At the Goldstone station, the dish used to receive these signals is 34 meters in diameter. This station received the signal of KPLO in July 2023 at a transmission power of $1 \cdot 10^{-13}$ W. This was the power of our faintest detection, and to date serves as a metric for the system's detection threshold, which is the faintest recorded signal. Using this DSN value as a metric of limitation, it was found that the limiting flux that this setup could substantially detect would be $1.03 \cdot 10^{-16}\, W/m^2$. By factoring in the collection area ratios of the two dishes (DSN v.s. our 0.6-m) the limiting power this setup can detect is $2.91 \cdot 10^{-17}\, W$. This number was acquired under the assumption the electromagnetic flux would be equivalent at both sites with the use of a hemispherical transmission profile. This detection threshold could be subject to change as a result of other conditions, such as inaccuracies with the recorded power on DSN Now, sensor temperature, bandwidth of the signal, and the noise profile in the frequency range and is only applicable for the LNA boosted frequency range of 2.1-2.5 GHz.

4. RESULTS

Figure 2 below shows an example of our detection in the form of a fast Fourier transform (FFT) plot, which has an intensity versus frequency display showing the downlink signal of the observed targets. The sharp "spike" located along the red line in the figure is a narrow bandwidth transmission occurring from the source. Below the detection is a waterfall plot showing an intensity versus time display where the time increases as you move downwards along the axis. See Fig. 2 displaying the specifics of the graphical display.

To determine if the detections were real and not just terrestrial strong, narrow bandwidth signals, we maneuvered our dish approximately 30 degrees away from the Moon to see if the signal disappeared. In each case, the signal vanished when the object was removed from the 3 dB beamwidth region of our dish, confirming that the signal is non-terrestrial.

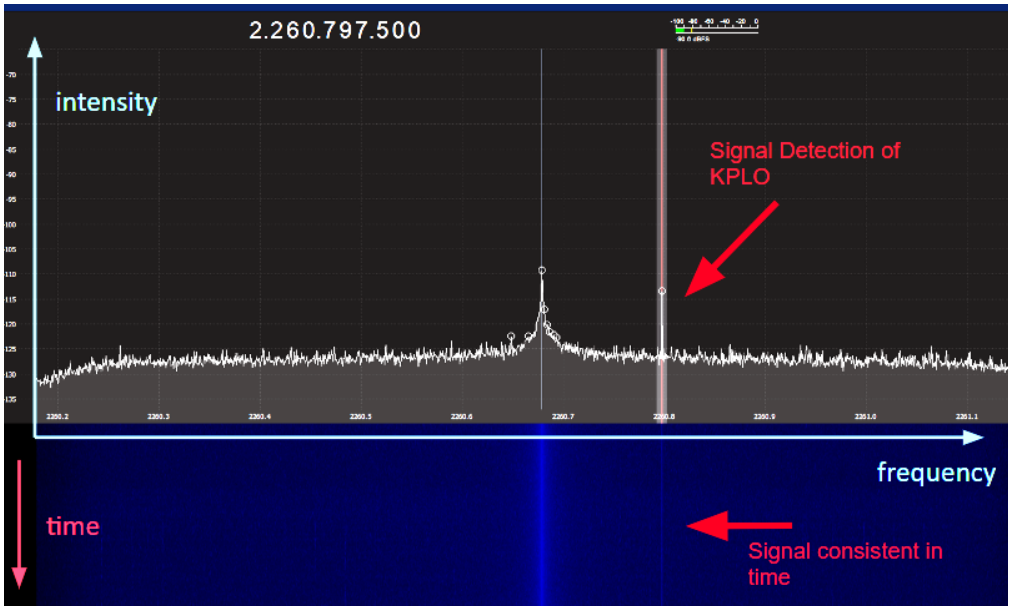

Fig. 2. Example FFT plot outputted as a GUI interface during the detection of KPLO's narrow bandwidth emission. Detection occurred at 2.26080 GHz with a magnitude of 17 dB above the noise floor. Bandwidth of the image is 0.5 MHz. Contrast is enhanced to see the signal constant in time displayed in the waterfall plot.

5. DISCUSSION

Through this survey we were able to successfully locate five cislunar targets with our prototype 0.6-meter passive RF dish system. While the astrometric precision of the 0.6-meter dish is not adequate for orbit determination due to its large beamwidth, a larger dish yields a smaller beamwidth that could provide significant tracking capabilities with this method. Additionally, a larger dish has the potential to reach fainter signals, increasing the distance limit for detections.

By performing this survey, we were able to determine our detection threshold by attempting observations of these cislunar targets. This detection threshold was found to be $2.91 \cdot 10^{-17}$ W in the LNA frequency boosted range of 2.1 to 2.5 GHz. This threshold does have the opportunity to change depending on the observation conditions, resulting in potentially fainter detections.

A typical Geosynchronous satellite has the energy capacity to transmit a maximum of 20 - 200 Watts of power [8]. Assuming that the antenna for a GEO satellite is a hemispherical emitter, this implies we could reliably detect this satellite at a distance of 170,000 - 538,000 kilometers, which is 1.4 times farther than the Moon, using the upper bound. The observations here have confirmed these calculations by successfully detecting five cislunar satellites at similar distances.

6. ACKNOWLEDGEMENTS

This research is supported by the State of Arizona Technology Research Innovation Fund and the Space Safety, Security and Sustainability Center (Space4) at the University of Arizona.

We respectfully acknowledge the University of Arizona is on the land and territories of Indigenous peoples. Today, Arizona is home to 22 federally recognized tribes, with Tucson being home to the O'odham and the Yaqui.

Committed to diversity and inclusion, the University strives to build sustainable relationships with sovereign Native Nations and Indigenous communities through education offerings, partnerships, and community service.

7. REFERENCES

[1] “Korean Pathfinder Lunar Orbiter.” *Nasa Space Sciences Data Coordinated Archive*, Accessed 31 July 2023.

[2] Hambleton, Kathryn. “Artemis I Map.” *NASA*, 9 Feb. 2018, www.nasa.gov/image-feature/artemis-i-map.

[3] Mars, Kelli. “Gateway.” *NASA*, 17 Aug. 2016, www.nasa.gov/gateway/overview.

[4] *Chandrayaan-3*, www.isro.gov.in/Chandrayaan3_New.html. Accessed 31 July 2023.

[5] Zhang, Jingrui, et al. “Leo Mega Constellations: Review of Development, Impact, Surveillance, and Governance.” *Space: Science & Technology*, vol. 2022, 30 July 2022, https://doi.org/10.34133/2022/9865174.

[6] “Chapter 3 Radio Telescopes and Radiometers.” *3 Radio Telescopes and Radiometers‣ Essential Radio Astronomy*, www.cv.nrao.edu/~sransom/web/Ch3.html. Accessed 31 July 2023.

[7] “Deep Space Services Catalog.” NASA Jet Propulsion Laboratory, 24 Feb. 2015.

[8] “SATELLITE SYSTEM CHARACTERISTICS TO BE CONSIDERED IN FREQUENCY SHARING ANALYSES BETWEEN GEOSTATIONARY-SATELLITE ORBIT (GSO) AND NON-GSO SATELLITE SYSTEMS IN THE FIXED-SATELLITE SERVICE (FSS) INCLUDING FEEDER LINKS FOR THE MOBILE-SATELLITE SERVICE (MSS).” International Telecommunication Union, 2000.